Orbital
The electronic journal of chemistry

the electronic journal of chemistry

**Full Paper** | http://dx.doi.org/10.17807/orbital.v17i2.21049

# A Study of Antioxidant Properties and a Pharmacokinetic Investigation of Chalcones and Pyrazolines

André Luis Kerek [a], Larissa Kozan [a], Gabrielle Schamne Fonseca [a], Bianca Sartori dos Santos [a], Raphaela Pereira Guaringue [a], Larissa Sens *[a], and Barbara Celânia Fiorin [a]

Antioxidant compounds are widely studied in the literature because they minimize oxidative damage in biological processes. In this context, chalcones and pyrazolines are considered prototype compounds for this purpose. This study describes the synthesis and characterization of seven compounds, including chalcones and pyrazolines, which were evaluated for their antioxidant power and pharmacokinetic properties. Compound **2b**, a pyrazoline with a para-substituted hydroxyl group, exhibited greater antioxidant activity compared to the other compounds in the study, thus showing good potential for future applications in biological activities.

## Graphical abstract

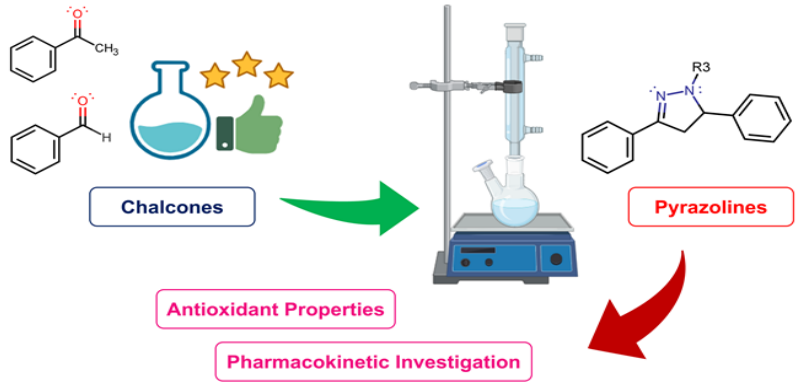


## Keywords

Antioxidant
Pharmacokinetics
Chalcones
Pyrazolines

## Article history

**Received** 01 May 2024
**Revised** 23 Oct 2024
**Accepted** 20 Dec 2024
**Available online** 19 May 2025

**Handling Editor:** Sergio R. Lazaro

## 1. Introduction

Currently, numerous studies are focused on seeking the discovery of new pharmacologically relevant compounds for the treatment of existing diseases and potential new illnesses, as exemplified by the case of SARS-CoV-2. In this scenario, certain classes of compounds have increasingly attracted the attention of researchers, such as chalcones and hybrids of this class with the pyrazole group, resulting in pyrazolines [1].

Pyrazolines are characterized by five-membered rings composed of three carbon atoms and two adjacent nitrogen atoms, along with an endocyclic double bond [2]. These possess various bioactive properties, including but not limited to antioxidant [3], anti-inflammatory [4], antiviral [5], antimicrobial [6, 7], antibacterial [8, 9], antitumor [10-13], and antituberculosis effects, particularly concerning conditions like rheumatoid arthritis and polyarthritis [14].

The biological activities of pyrazolines are of significant interest in pharmacokinetics, a central field in the development of new drugs, which analyzes the distribution of medications in the body from their initial absorption to metabolism and excretion processes. Consequently, through

[a] Department of Chemistry, State University of Ponta Grossa -UEPG, Av. General Carlos Cavalcanti, 4748, zip code - 84030-900- Ponta Grossa, Paraná, Brazil. *Corresponding author. E-mail: **larissasens@hotmail.com**

this analysis, it is possible to determine therapeutic efficacy, medication safety, enhance its formulation [15], and determine the percentage of the dose available in the body.

The concept of bioavailability is crucial in pharmacokinetics and is associated with the mode of medication administration, as well as its absorption in the gastrointestinal tract, metabolism in the liver, drug interactions, and the physiological and pathological state of the patient [16]. Understanding medication bioavailability is essential for the correct prescription of pharmaceutical products, as its efficacy is directly influenced by this factor, being essential to ensure optimal therapeutic results and avoid negative side effects [17]. Therefore, the search for new molecules to assist in pharmaceutical industry innovations is becoming increasingly prevalent, with its study associated with medicinal chemistry [18].

In literature, there are several synthetic routes for obtaining pyrazolines using different reagents, with one of the options being the cyclization of α,β-unsaturated chalcones with hydrazines and derivatives.

Considering the relevance of pyrazolines as compounds with biological potential, as well as the diversity of synthetic approaches described in the literature, the central objective of this study is the synthesis, evaluation of pharmacokinetic properties, and antioxidant activity of chalcones and pyrazolines.

## 2. Results and Discussion

*Synthesis and Characterization*

The synthesis of the pyrazolines detailed in this study involved the initial preparation of chalcones **1a-c**, followed by their isolation and characterization. The first synthetic step was carried out via a Claisen-Schmidt condensation, where equimolar amounts of acetophenones and benzaldehydes are reacted using a basic catalyst. Following that, to obtain pyrazolines **2a-c** and **3a**, the chalcones were cyclized by reacting with hydrazine using acetic acid as a solvent, thus, the pyrazolines obtained were acetylated. Pyrazoline **3a** was obtained by reacting chalcones with phenylhydrazine. In Scheme 1, it is possible to observe the compounds that were synthesized, as well as the synthetic route used in this work.

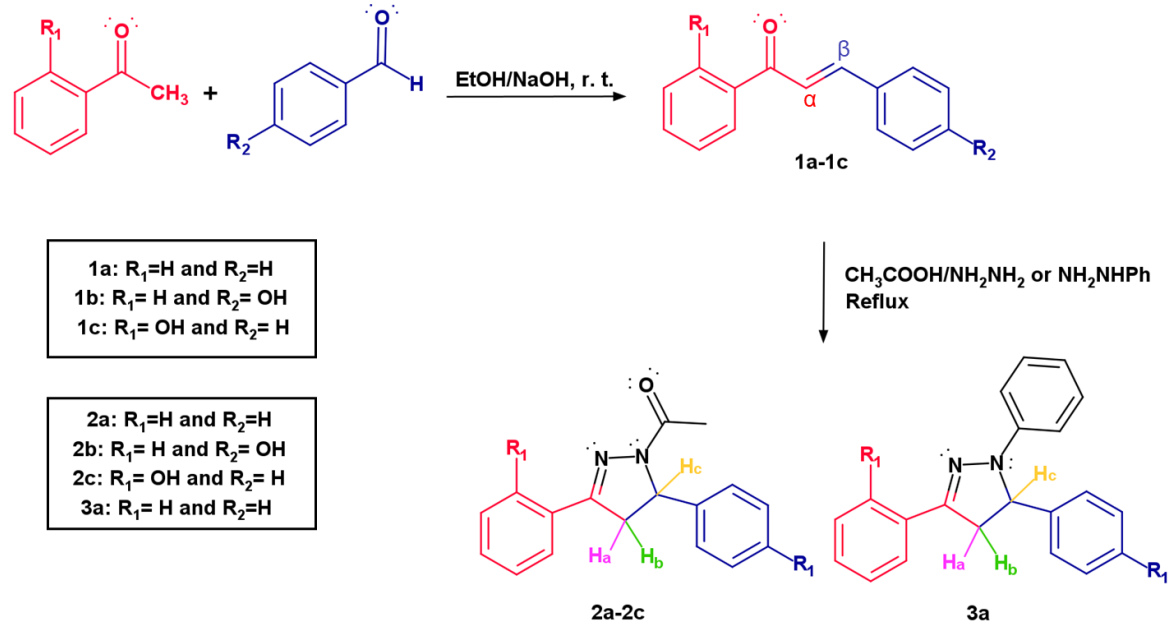


**Scheme 1.** Synthesis of chalcones and pyrazolines.

All synthesized compounds were characterized by melting point (mp), Infrared (IR), $^{1}H$ and $^{13}C$ Nuclear Magnetic Resonance (NMR). Heteronuclear Multiple Bond Correlation (HMBC) and Heteronuclear Single Quantum Coherence (HSQC) spectroscopy were performed for the pyrazolines. In the supplementary material, it is possible to observe all the spectra of chalcones **1a-c** (Figure S1-S3, S8-S10 and S23-S25) and pyrazolines **2a-c** and **3a** (Figure S4-S7, S11-S14, S15-S22 and S26-S29).

In the $^{1}H$ NMR spectrum, it was possible to identify the characteristic signals of the heterocyclic ring of pyrazolines, which appear as double doublets in the regions of 3.19 - 3.26 ppm, 3.62 - 3.91 ppm and 5.47 - 5.63 ppm. The hydrogens corresponding to the formation of pyrazoline are presented as double doublets, as there are methylene hydrogens neighboring an asymmetric carbon, which gives it the characteristic of diasterotopic hydrogens, thus, the vicinal coupling constants can be observed ($^{3}J_{ac}$= 4.6 Hz and $^{3}J_{bc}$= 11.8 Hz) and geminal ($^{2}J_{ab}$= 17.7 Hz).

To assign the signals of the pyrazoline carbons, the $^{13}C$ NMR, HSQC and HMBC spectra of the pyrazolines were analyzed. It was observed that carbon at around 59.9 ppm correlates with hydrogen at 5.60 ppm ($H_c$), carbon at around 42.4 ppm correlates with hydrogen at 3.74 ppm ($H_b$) and 3.16 ppm ($H_a$), carbon at around 154.0 ppm is defined as the carbon of the $sp^2$ hybridized heterocycle. Furthermore, for pyrazolines **2a-c** the carbonyl carbon is found to be around 169.0 ppm, this is because these pyrazolines are acetylated, however, the presence of a carbonyl carbon of pyrazoline **3a** is not observed, since for the Its preparation uses phenylhydrazine. Signals between 100-155 ppm are attributed to aromatic carbons.

Furthermore, infrared was used to identify the characteristic bands of hydroxyl, amide, double bond between carbon and nitrogen, varying according to the specific

structure of each compound. In the FT-IR spectrum, the bands between 3040-3063 $cm^{-1}$ refer to the stretching of the C-H bonds in aromatic rings. Additionally, the C-H stretching peaks for $sp^3$-hybridized carbon can be observed nearby. An intense band was also observed in the region of 1700 $cm^{-1}$, which refers to the vibration of the C=O bond, resulting from the presence of the carbonyl group in pyrazolines **2a-c**. The bands that appear around 1300 $cm^{-1}$ are related to the formation of pyrazoline, resulting from the C-N chemical bond.

*Pharmacokinetic analysis*

The chalcones and pyrazolines discussed in this work (Scheme 1) were subjected to *in silico* analysis on the SwissADME online platform to evaluate the pharmacokinetic properties. In this way, the physicochemical properties of organic compounds were obtained (Table 1 and Table S1), which are essential for estimating characteristics such as absorption based on molecular mass and topological polar surface area (TPSA).

**Table 1.** Physicochemical properties of synthesized chalcones and pyrazolines.

| Compound | MW (g.mol$^{-1}$) | NRBs | NHBAs | NHBDs | TPSA (Ã$^2$) | Consensus Log $P_{o/w}$ | Bioavailability |
|---|---|---|---|---|---|---|---|
| **1a** | 208.26 | 3 | 1 | 0 | 17.07 | 3.29 | 0.55 |
| **1b** | 224,25 | 3 | 2 | 1 | 37.30 | 2.87 | 0.55 |
| **1c** | 224.25 | 3 | 2 | 1 | 37.30 | 3.13 | 0.55 |
| **2a** | 264.32 | 3 | 2 | 0 | 32.67 | 2.85 | 0.55 |
| **2b** | 280.32 | 3 | 3 | 1 | 52.90 | 2.44 | 0.55 |
| **2c** | 280.32 | 3 | 3 | 1 | 52.90 | 2.51 | 0.55 |
| **3a** | 298.38 | 3 | 1 | 0 | 15.60 | 4.26 | 0.55 |

MW: Molecular Weight, NRBs: number of rotatable bonds, NHBAs: number of hydrogen bond acceptors, NHBDs: number of hydrogen bond donors, TPSA: topological surface area, Log $P_{o/w}$: octanol-water partition coefficient.

Lipinski's rule is widely used when analyzing the oral bioavailability of potential drugs. A compound is considered viable in terms of its bioavailability when it obeys at least three of the defined rules: molecular weight ≤ 500 Daltons, hydrogen bond acceptor (HBA) ≤ 10, hydrogen bond donor (HBD) ≤ 5, lipophilicity (Log P) ≤ 5. Therefore, considering the Lipinski criteria, the mass values do not exceed 500 g mol $^{-1,}$ the octanol-water partition coefficient is less than 5, the number of hydrogen bond acceptor and donor groups does not exceed 5 and 10, respectively [19-20]. Furthermore, the polar surface area does not exceed 140 Å [21].

In addition to Lipinski's rule, other parameters were evaluated to verify the viability of organic compounds - Ghose, Veber, Egan and Muegge, as demonstrated in Table S1. With the analysis of the factors mentioned above, it becomes evident that compounds **1a-3a** present excellent oral absorption, as they adhere to the parameters of all authors.

On the other hand, compound **3a** does not adhere to a Lipinski criterion determined by the SwissADME analysis system, which creates an alert when the Log $P_{o/w}$ (MLOGP) is greater than 4.15, for pyrazoline **3a** the value obtained for MLOGP was 4.46. The same compound also violates a Muegge criterion, obtaining a Log $P_{o/w}$ (XLOGP3) of 5.02. However, there are reports in the literature that establish values of Log P ≤ 5 as one of the Lipinski criteria 20 [19-20]. Moreover, although it is acknowledged that one of the criteria is violated, while the others are met, compound **3a** should not be discarded. Furthermore, the consensus values Log $P_{o/w}$ is > 2 and < 5, which represent that the compounds will have good absorption, distribution, metabolism and excretion characteristics. Overall, all compounds presented a bioavailability score of 0.55, which represents that compounds can act as good oral drugs [19].

Additionally, the diagrams depicted in Figure 1 illustrate the bioavailability radar generated from the physicochemical properties of the compounds. Among the six parameters evaluated—molecule size, solubility, polarity, saturation, flexibility, and lipophilicity—five remained within the ideal range, depicted by the region in red. However, it was observed that each compound exhibits distinct molecular behavior. Therefore, a variety of parameters are necessary to comprehend all potential reactions and effects in the body.

The pharmacokinetic characteristics of gastrointestinal (GI) absorption, blood-brain barrier (BBB) permeability and P-Glycoprotein (P-gp) inhibition of the synthesized chalcones and pyrazolines are presented in Table 2. The high gastrointestinal absorption suggests that the compounds will be broken down and digested quickly in the body, being largely absorbed by the small intestine. As for the blood-brain barrier (BBB), which controls the interaction between the blood and the brain; the high result indicates that the compounds can penetrate the central nervous system (CNS), suggesting their possible use in the treatment of CNS infections [19, 22, 23]. Upon analyzing these factors, it was observed that all compounds examined meet the criteria deemed ideal for drug characteristics. They exhibit high gastrointestinal absorption, enhancing their uptake by the organism, while simultaneously demonstrating permeation across the blood-brain barrier, rendering them effective in addressing existing CNS pathologies.

**Table 2.** Pharmacokinetic properties of gastrointestinal (GI) absorption, blood-brain barrier (BBB) and P-glycoprotein (P-gp) permeability.

| Compound | GI | BBB | P-gp |
|---|---|---|---|
| **1a** | High | Yes | No |
| **1b** | High | Yes | No |
| **1c** | High | Yes | No |
| **2a** | High | Yes | No |
| **2b** | High | Yes | No |
| **2c** | High | Yes | No |
| **3a** | High | Yes | No |

In relation to the substrate analysis of P-glycoprotein (P-gp), none of the compounds exhibited this activity, which is an intriguing observation. This glycoprotein, predominantly located in the gastrointestinal tract, liver, and kidneys, facilitates the transport of substances for elimination from the organism. Therefore, this finding is considered favorable, as it enables P-gp to maintain its functionality, preventing the accumulation of substances in metabolism and thereby averting drug intoxication or overdose [24].

Table 3 shows the results corresponding to the inhibition with the following cytochromes were evaluated: CYP1A2 (caffeine, aflatoxin B, paracetamol metabolism); CYP2C19

(omeprazole, mephenytoin, diazepam metabolism); CYP2C9 (warfarin, losartan, some anti-inflammatories metabolism); CYP2D6 (neurosteroids and serotonin metabolism); and CYP3A4 (one of the main drug-metabolizing enzymes) [25, 26]. These enzymes, known as monooxygenases, are related to the reaction and process of drug metabolism in the liver.

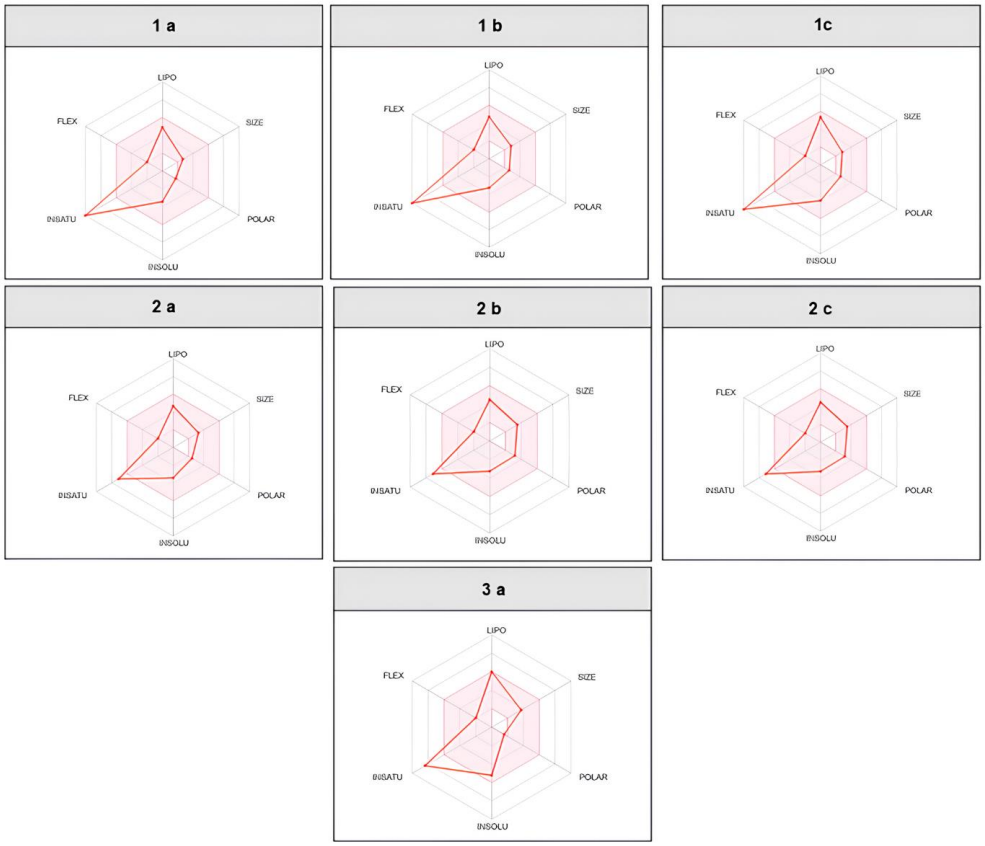


**Fig.1.** Bioavailability radar of the analyzed compounds.

**Table 3.** Pharmacokinetic properties of isoenzyme inhibition.

| Compound | CYP1A2 inhibitor | CYP2C19 inhibitor | CYP2C9 inhibitor | CYP2D6 inhibitor | CYP3A4 inhibitor |
|---|---|---|---|---|---|
| **1a** | No | Yes | No | No | No |
| **1b** | No | Yes | No | No | No |
| **1c** | No | Yes | Yes | No | No |
| **2a** | No | Yes | Yes | No | No |
| **2b** | No | No | No | No | No |
| **2c** | No | Yes | No | No | No |
| **3a** | Yes | Yes | Yes | Yes | No |

The data analysis regarding CYP inhibition can be interpreted in two ways. The first applies to specific cases, such as when there's a well-defined target or when acting as a prodrug. In this scenario, inhibiting these cytochromes would make another drug more available to exert its mechanism of action, albeit potentially increasing its side effects. The second scenario arises when cytochromes are not inhibited, allowing for the normal metabolism of drugs for elimination. While this may require higher doses of the compound, it reduces the likelihood of drug interactions with other xenobiotic compounds [25, 27].

The synthesized compounds showed varied results in CYP inhibition. Most chalcones (**1a-c**) inhibited the first three cytochromes and not the other two. Pyrazolines (**2a-c** and **3a**) mostly inhibited only two cytochromes, except for compound **3a**, which didn't inhibit CYP3A4, suggesting lower pharmacological potential. Conversely, compound **2b** showed the best results in pharmacokinetic properties evaluations, not inhibiting any cytochrome tested *in silico*, indicating good pharmacological potential.

In the analysis of the Brain Or IntestinaL EstimateD permeation (BOILED-Egg) method (Figure 2), a graphical representation is used to illustrate whether compounds exhibit both factors mentioned, namely the Absorption in Gastrointestinal tract (AGI) and Blood-Brain Barrier Permeation (BHE). If a compound is situated in the "yolk" region, it indicates both high AGI and permeability through the blood-brain barrier. Conversely, if the compound is in the "white" region, it denotes only high AGI [28].

*Antioxidant activity*

The antioxidant activity was carried out through the inhibition of the DPPH radical, for this the radical inhibition power was evaluated against chalcones and pyrazolines, in concentrations that varied from 50 mM to 200 mM, and compared with a 3.3 mM solution of quercetin, with ethanol as solvent, and in all analyzes triplicates were performed.

The pyrazolines obtained a better antioxidant activity than the chalcones, with **2b** being the one that presented the best result, with an $IC_{50}$ value of 12.6 mM, followed by **2c** with 33.8 mM, **3a** with 38.8 mM and **2a** with 46.2 mM. As for chalcones, compound **1b** presented the best $IC_{50}$ result of 240.9 mM, followed by chalcones **1a** and **1c** which presented values greater than 300 mM.

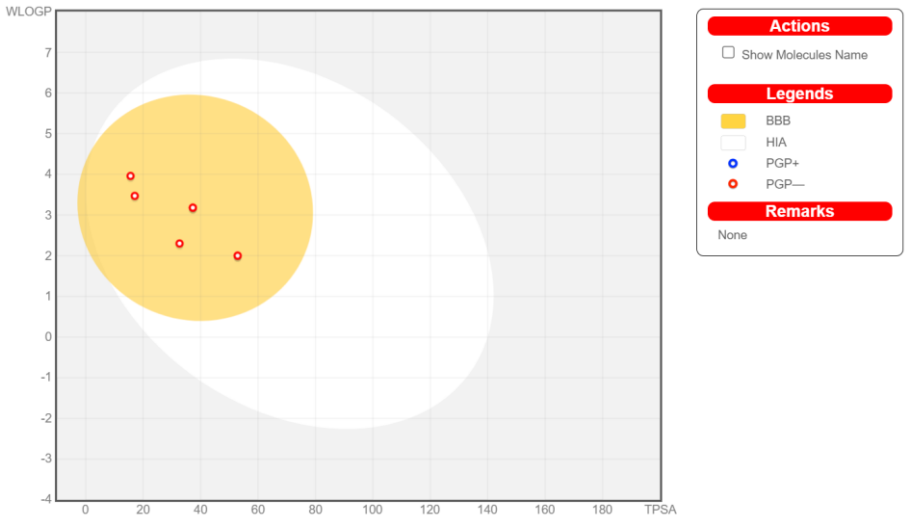


**Fig. 2.** BOILED-Egg Graph.

**Table 4**. $IC_{50}$ results for DPPH radical inhibition.

| Compound | $IC_{50}$ (mM) |
|---|---|
| **1a** | > 300.0 |
| **1b** | 240.9 |
| **1c** | > 300.0 |
| **2a** | 46.2 |
| **2b** | 12.6 |
| **2c** | 33.8 |
| **3a** | 38.0 |

With the results obtained in this study, it was possible to verify that the cyclization of chalcones enhanced their antioxidant potential. This can be explained by the insertion of the pyrazolinic ring in their structure. When analyzing the mechanisms of action of antioxidants against the DPPH radical, it appears that there are two modes of action: by electron transfer, or donation of H atoms [29]. As pyrazolines have two nitrogens with lone pairs of electrons, this explains the increase in its antioxidant potential.

Upon analyzing the substituents among chalcones **1a-c**, it was anticipated that the phenolic compounds would yield the best results when evaluating their antioxidant activity against the DPPH radical, however the highlighted result was for chalcone **1b**, which presents the hydroxyl group at position 4, making it more available to react with the DPPH radical when compared to phenolic chalcone **1c**, since its hydroxyl may be making intramolecular hydrogen bonds with the carbonyl, therefore, it is less available, a fact that may justify the result obtained.

The same profile is observed when the pyrazoline substituents are analyzed, that is, for compound **2b**, it is added to the fact that the hydroxyl is in position 4 with the presence of the pyrazole ring, resulting in the most active compound found in this work.

Furthermore, compound **2b** exhibits bioavailability factors that enhance its attractiveness. It demonstrates high gastrointestinal absorption and suggests a good ability to penetrate the CNS. Additionally, it is noteworthy that the compound appears to be a non-substrate for P-glycoprotein and does not seem to act as an isoenzyme inhibitor.

## 3. Material and Methods

*General procedure for the synthesis of chalcones*

The chalcones **1a-c** (Scheme 1) were synthesized in a round-bottom flask, where a solution of 50.0 mL of ethyl alcohol with the corresponding acetophenone (10.0 mmol) was prepared. Immediately thereafter, the respective aldehyde (10.0 mmol) was added, followed by a solution of 4.0 mL of NaOH (50%), the basic catalyst for the reaction. After this process, the reaction was maintained under magnetic stirring for 24 hours. Subsequently, the reaction was acidified with a 1:1 HCl solution. The resulting compounds were extracted with dichloromethane, followed by evaporation of the solvent using a rotary evaporator [30,31]. The samples were dried in a desiccator before the necessary characterizations were carried out.

*General procedure for the synthesis of pyrazolines*

The compounds **2a-c** and **3a** (Scheme 1) were synthesized in a round-bottomed flask containing 10.0 mL of acetic acid. To this was added 1.0 mmol of the chalcone and 3.0 mmol of hydrazine (**2a-c**) or 3.0 mmol of phenylhydrazine (**3a**). The reaction mixture was kept at reflux with magnetic stirring for approximately 12 hours. After that, the reaction was poured onto ice and the precipitate was vacuum filtered. Finally, the product was purified by recrystallization using ethyl alcohol as a solvent [32].

*Characterization*

The compounds were characterized using $^{1}H$ and $^{13}C$ NMR spectroscopy on a Bruker 400 MHz AVANCE III nuclear magnetic resonance spectrometer (operating at 400 MHz for $^{1}H$ and 100 MHz for $^{13}C$). Approximately 20 mg of the compound was solubilized in tetramethylsilane (TMS) as an internal reference and the temperature of the probe was kept close to 25.0°C. In addition, FT-IR analyses were carried out on a Shimadzu FT-IR Prestige-21 spectrometer. The samples were prepared in potassium bromide (KBr) pellets and the equipment was operated at 64 scans with a resolution of 2 $cm^{-1}$. The range analyzed was 400 - 4000 $cm^{-1}$. Ultimately, the melting point was determined employing a digital melting point apparatus MQAPF-301, with a heating rate of 1.0°C per minute.

**(2*E*)-1,3-diphenylprop-2-en-1-one (1a):** Pale yellow solid, **Yield**: 63%, **m.p**: 53.5 °C, **FT-IR (KBr, $cm^{-1}$)**: 3061, 1660, 1610. **$^{1}H$ NMR ($CDCl_3$, 400 MHz)**: δ 8.02 (1H, d, H-2' and H-6'), 7.82

(1H, d, $^3J$ = 15.7 Hz, Hβ), 7.65 (2H, m, H-2 and H-6), 7.59 (1H, m, H-4'), 7.54 (1H, d, $^3J$ = 15.7 Hz, Hα), 7.49 (2H, m, H-3' and H-5'), 7.42 (3H, m, H-3, H-4 and H-5), **$^{13}$C NMR ($CDCl_3$, 100 MHz)**: δ 190.6 (C=O), 144.9 (Cβ), 138.2, 134.9, 132.8, 130.6, 130.0, 128.7, 128.5, 128.4, 122.1 (Cα).

**(2*E*)-3-(4-hydroxyphenyl)-1-phenylprop-2-en-1-one (1b):** Yellow solid, **Yield**: 51%, **m.p**: 186.3 °C, **FT-IR (KBr, cm$^{-1}$)**: 3320, 1649, 1599. **$^1$H NMR ($CDCl_3$, 400 MHz)**: δ 8.01 (2H, d, H-2' and H-6'), 7.78 (1H, d, $^3J$ = 15.6 Hz, Hβ), 7.58 (3H, m, H-2, H-6 and H-4'), 7.50 (2H, t, H-3' and H-5'), 7.41 (1H, d, $^3J$ = 15.6 Hz, Hα), 6.89 (2H, d, H-3 and H-5), 5.41 (1H, OH), **$^{13}$C NMR ($CDCl_3$, 100 MHz)**: δ 190.8 (C=O), 157.9 (OH), 144.8 (Cβ), 138.4, 132.6, 130.5, 128.6, 128.4, 127.8, 119.9 (Cα), 116.0.

**(2*E*)-1-(2-hydroxyphenyl)-3-phenylprop-2-en-1-one (1c):** Yellow solid, **Yield**: 29%, **m.p**: 87.6 °C, **FT-IR (KBr, cm$^{-1}$)**: 3030, 1639, 1572. **$^1$H NMR ($CDCl_3$, 400 MHz)**: δ 12.81 (1H, OH), 7.94 (2H, m, $^3J$ = 15.4 Hz, Hβ), 7.67 (3H, m, $^3J$ = 15.3 Hz, Hα), 7.51 (1H, t, H-4'), 7.45 (3H, m, H-6', H-3 and H-5), 7.04 (1H, d, H-3'), 6.96 (1H, t, H-5'), **$^{13}$C NMR ($CDCl_3$, 100 MHz)**: δ 193.8 (C=O), 163.6 (OH), 145.5 (Cβ), 136.4, 134.6, 130.9, 129.7, 129.1, 128.7, 120.2 (Cα), 120.0, 118.9, 118.7.

**1-(3,5-diphenil-4,5-dihydro-1H-pyrazol-1-yl)ethan-1-one (2a):** Yellow solid, Yield: 65%, **m.p:** 131.4 °C, **FT-IR (KBr, cm$^{-1}$):** 2940, 1651, 1596. **$^1$H NMR ($CDCl_3$, 400 MHz):** d 7,74 (3H, m, Ar), 7,42 (4H, m, Ar) 7,33 (3H, m, Ar), 7,23 (3H, m, Ar), 5,60 ($^1$H, dd, $H_C$, $^3J_{CA}$ = 4,6 Hz, $^3J_{CB}$ = 11,8 Hz), 3,74 (1H, dd, $H_B$, $^2J_{BA}$ = 17,7 Hz, $^3J_{BC}$ = 11,8 Hz), 3,16 (1H, dd, $H_A$, $^2J_{AB}$ = 17,7 Hz, $^3J_{AC}$ = 4,6 Hz), 2.43 (3H, s, $CH_3$). **$^{13}$C NMR ($CDCl_3$, 100 MHz):** d 168.9 (C=O), 153.9 (Cg), 141.8, 131.4, 130.3, 128.9, 128.7, 127.6, 126.6, 125.6, 59.9 (Cb), 42.4 (Ca), 21.9 ($CH_3$).

**1-[5-(4-hydroxyphenil)-3-phenil-4,5-dihydro-1H-pyrazol-1-yl]ethan-1-one (2b):** Pale yellow solid, **Yield:** 49%, **m.p:** 146.3 °C, **FT-IR (KBr, cm$^{-1}$):** 3286, 3039, 1647, 1594. **$^1$H NMR ($CDCl_3$, 400 MHz):** d 8.67 (1H, s, OH) 7.73 (2H, m, Ar), 7.42 (4H, m, Ar) 7.37 (4H, m, Ar), 7.05 (2H, m, Ar), 6.78 (2H, m, Ar), 5.51 (1H, dd, $H_C$, $^3J_{CA}$ = 4,2 Hz, $^3J_{CB}$ = 11,7 Hz), 3.72 (1H, dd, $H_B$, $^2J_{BA}$ = 17,7 Hz, $^3J_{BC}$ = 11,7 Hz), 3.15 (1H, dd, $H_A$, $^2J_{AB}$ = 17,7 Hz, $^3J_{AC}$ = 4,2 Hz), 2.39 (3H, s, $CH_3$). **$^{13}$C NMR ($CDCl_3$, 100 MHz):** d 168.7 (C=O), 156.7 (OH), 154.0 (C g), 132.7, 131.5, 130.2, 128.7, 126.8, 126.6, 59.5 (Cb), 42.4 (Ca), 22.0 ($CH_3$).

**1-[3-(2-hydroxyphenil)-5-phenil-4,5-dihydro-1H-pyrazol-1-yl]ethan-1-one (2c):** Yellowish solid, **Yield:** 21%, **m.p:** 138.9 °C, **FT-IR (KBr, cm$^{-1}$):** 3159, 3044, 1650, 1598. **$^1$H NMR ($CDCl_3$, 400 MHz):** d 10,27 (1H, s, OH), 7,34 (3H, m, Ar), 7,25 (4H, m, Ar) 7,06 (1H, d, Ar), 6,93 (1H, t, Ar), 6,78 (2H, m, Ar), 5,57 (1H, dd, $H_C$, $^3J_{CA}$ = 4,7 Hz, $^3J_{CB}$ = 11,9 Hz), 3,86 (1H, dd, $H_B$, $^2J_{BA}$ = 17,8 Hz, $^3J_{BC}$ = 11,9 Hz), 3,30 (1H, dd, $H_A$, $^2J_{AB}$ = 17,8 Hz, $^3J_{AC}$ = 4,7 Hz), 2,38 (3H, s, $CH_3$). **$^{13}$C NMR ($CDCl_3$, 100 MHz):** d 167.8 (C=O), 157.7 (OH), 156.4 (Cg), 141.2, 132.3, 129.1, 128.4, 128.0, 125.6, 119.8, 117.1, 115.1, 58.5 (Cb), 42.7 (Ca), 22.1 ($CH_3$).

**1,3,5-triphenil-4,5-dihydro-1H-pyrazol (3a):** Beige solid, **Yield:** 84%, **m.p:** 137.6 °C, **FT-IR (KBr, cm$^{-1}$):** 3038, 1597. **$^1$H NMR ($CDCl_3$, 400 MHz):** d 8.02 (1H, d, Ar), 7,72 (2H, m, Ar), 7,54 (2H, m, Ar) 7,39 (3H, m, Ar), 7,25 (2H, m, Ar), 7,17 (2H, t, Ar), 7,07 (2H, m, Ar), 6,77 (1H, t, Ar), 5,27 (1H, dd, $H_C$, $^3J_{CA}$ = 7,3 Hz, $^3J_{CB}$ = 12,4 Hz), 3,84 (1H, dd, $H_B$, $^2J_{BA}$ = 17,1 Hz, $^3J_{BC}$ = 12,4 Hz), 3,14 (1H, dd, $H_A$, $^2J_{AB}$ = 17,1 Hz, $^3J_{AC}$ = 7,3 Hz). **$^{13}$C NMR ($CDCl_3$, 100 MHz):** d 146,7 (Cg), 142.6, 138.2, 134.9, 132.8, 129.0 – 125.0 (Ar), 119.1, 113.4, 64.5 (Cb), 43.6 (Ca).

### *Pharmacokinetic analysis*

The *SwissADME online* platform was used for the pharmacokinetic analysis. This platform gathers promising parameters for chalcones and pyrazolines, such as physicochemical properties, oral administration, lipophilicity, solubility and pharmacokinetics. In addition, Lipinski's rules and their extensions were used to analyze the results.

### *Antioxidant activity*

The antioxidant activity was evaluated using the DPPH radical inhibition methodology, which initially involves adding 160.0 µL of a 1.5 mM DPPH solution to a microplate, followed by the addition of 40.0 µL of the sample solutions (**1a-d**, **2a-c** and **3a**) at concentrations ranging from 50.0 mM to 200.0 mM. The mixture was then allowed to incubate in a light-free environment for 30 minutes. Subsequently, the absorbance was measured at a wavelength of 517 nm, following the methodology outlined by Hamlaoui and collaborators (2018) [33]. A standard solution of 1.0 mM quercetin, a well-known antioxidant in the literature, was employed as a positive control.

## 4. Conclusions

In this article, we report the synthesis and characterization of three chalcones and four pyrazolines. The chalcones were synthesized via Claisen-Schmidt condensation, while the pyrazolines were obtained by cyclizing the chalcones with hydrazine or phenylhydrazine. The synthesized compounds were characterized using FT-IR and NMR techniques.

All compounds were subjected to DDPH radical inhibition assays, which is a good parameter for evaluating antioxidant activity. Given that compound **2b** stood out from the others by presenting an $IC_{50}$ of 12.6 mM, the explanation for this result can be attributed to the presence of the pyrazolinic ring and the hydroxyl in position 4.

In addition, all compounds were evaluated for their pharmacokinetic parameters, where it was found that high gastrointestinal absorption and suggests a good ability to penetrate the CNS. Additionally, it is noteworthy that the compound appears to be a non-substrate for P-glycoprotein and does not seem to act as an isoenzyme inhibitor.

## Supporting Information

Supplementary data to this article can be found online.

## Acknowledgments

This work was supported by Brazilian National Council for Scientific and Technological Development (CNPq) and Brazilian Federal Agency for Support and Evaluation of Graduate Education (CAPES). Furthermore, the authors are thankful to Institutional Laboratory C- LABMU/UEPG for the use of the characterization facilities.

## Author Contributions

André Luis Kerek: Data curation, Investigation, Writing – original draft. Larissa Kozan: Data curation, Formal Analysis, Visualization, Writing – original draft. Gabrielle Schamne Fonseca: Data curation, Investigation, Writing – original draft. Bianca Sartori dos Santos: Data curation, Investigation, Writing – original draft. Raphaela Pereira Guaringue: Data curation, Investigation, Formal Analysis. Larissa Sens: Conceptualization, Funding acquisition, Supervision, Writing – review & editing. Barbara Celânia Fiorin: Conceptualization, Funding acquisition, Resources, Supervision, Writing – review & editing.

## References and Notes


[1] Uddin, M. N. et. al. *Results Chem.* **2022**, *4*, 1. [Crossref]

[2] Vahedpour, T.; Hamzeh-Mivehroud, M.; Hemmati, S.; Dastmalchi, S. *ChemistrySelect* **2021**, *6*, 6483. [Crossref]

[3] Raut, D. G.; Lawand, A. S.; Kadu, V. D.; Hublikar, M. G.; Patil, S. B.; Bhosale, D. G.; Bhosale, R. B. *Polycyclic Aromat. Compd.* **2022**, *42*, 70. [Crossref]

[4] Abdellatif, K. R. A.; Elshemy, H. A. H.; Azoz, A. A. *Bioorg. Chem.* **2015**, *63*, 13. [Crossref]

[5] Manna, F.; Chimenti, F.; Fioravanti, R. et al. *Bioorg. Med. Chem. Lett.* **2005**, *15*, 4632. [Crossref]

[6] Harikrishna, N.; Isloor, A. M.; Ananda, K.; Obaid, A.; Fun, H. K. *New J. Chem.* **2016**, *40*, 73. [Crossref]

[7] Nisa, S.; Yusuf, M. *J. Heterocycl. Chem.* **2020**, *57*, 2024. [Crossref]

[8] Khan, S. A.; Asiri, A. M.; Kumar, S.; Sharma, K. *Eur. J. Chem.* **2014**, *5*, 85. [Crossref]

[9] Viveka, S.; Dinesha; Shama, P.; Nagaraja, G. K.; Ballav, S.; Kerkar, S. *Med. Chem.* **2015**, *101*, 442. [Crossref]

[10] Nepali, K.; Kadian, K.; Ojha, R.; Dhiman, R.; Garg, A.; Singh, G.; Buddhiraja, A.; Bedi, P. M. S.; Dhar, K. L. *Med. Chem. Res.* **2012**, *21*, 2990. [Crossref]

[11] Karabacak, M.; Altintop, M. D.; Çiftçi, H. I.; Koga, R.; Otsuka, M.; Fujita, M.; Özdemir, A. *Molecules* **2015**, *20*, 19066. [Crossref]

[12] Chouiter, M. I.; Boulebd, H.; Pereira, D. M.; Valentão, P.; Andrade, P. B.; Belfaitah, A.; Silva, A. M. S. *Future Med. Chem.* **2020**, *12*, 493. [Crossref]

[13] Nawaz, F.; Alam, O.; Perwez, A. ; Rizvi, M. A.; Naim, M. J.; Siddiqui, N.; Pottoo, F. H.; Jha, M. *Archiv der Pharmazie* **2020**, *353*, 1900262. [Crossref]

[14] Raghav, N.; Sing, M. *Bioorg. Med. Chem.* **2014**, *22*, 4233. [Crossref]

[15] Steinkellner, A.; Chen, W.; Denison, S. E. *Am. J. Med.* **2010**, *123*, 929. [Crossref]

[16] Consiglieri, V. O.; Storpirtis, S. *Rev. Bras. Cienc. Farm.* **2000**, *36*, 13. [Link]

[17] Pedrazzoli Júnior, J. et al. *RBM Rev. Bras. Med.* **2013**, 70, 82.

[18] Holbrooka, S. L. Y.; Tsodikova, S. G. *MedChemComm* **2017**, *8*, 1739. [Crossref]

[19] Okolo, E. N.; Ugwu, D. I.; Ezema, B. E. et al. *Sci. Rep.* **2021**, *11*, 1. [Crossref]

[20] Lipinski, C. A.; Lombardo, F.; Dominy, B. W.; Feeney, P. J. *Adv. Drug Deliv. Rev.* ***2001***, *46*, 3. [Crossref]

[21] Barret, R. 5 - Importance and Evaluation of the Polar Surface Area (PSA and TPSA), Editor: Roland Barret, Therapeutical Chemistry, Elsevier, 2018, Pages 89-95, ISBN 9781785482885. [Crossref]

[22] Bandaru, V. et. al. *J. Mol. Struct.* **2024**, *1309*, 138149. [Crossref]

[23] Hasan, A. H. et al. *Bioorg. Chem.* **2022**, *119*, 105572. [Crossref]

[24] Fayed, E. A. et al. *J. Mol. Struct.* **2021**, *1234*, 130. [Crossref]

[25] Feyereisen, R. 8 - Insect CYP Genes and P450 Enzymes, Editor: Gilbert, L. I. Insect Molecular Biology and Biochemistry, Academic Press, 2012, Pages 236-316, ISBN 9780123847478. [Crossref]

[26] MCMillan, D. M.; Tyndale, R. F. *Pharmacol. Ther.* **2018**, *184*, 189. [Crossref]

[27] Zhao, L. et al. *Bioorg. Med. Chem. Lett.* **2019**, *29*, 2016. [Crossref]

[28] Daina, A.; Zoete, V. *ChemMedChem* **2016,** *11*, 1117. [Crossref]

[29] Gulcin, I.; Alwasel, S. H. *Processes* **2023**, *11*, 2248. [Crossref]

[30] Yazdan, S. K. et al. *J. Appl. Chem. (Lumami, India)* **2014**, *3*, 601.

[31] Marocviz, C. et al. *J. Mol. Struct.* **2022**, *1258,* 132647. [Crossref]

[32] Machado, V. et al. *RSC Med. Chem.* **2022**, *312*, 1644. [Crossref]

[33] Hamlaoui, I. et al. *J. Mol. Struct.* **2018**, *1156*, 385. [Crossref]


## How to cite this article

Kerek, A. L.; Kozan, L.; Fonseca, G. S.; dos Santos, B. S.; Guaringue, R. P.; Sens, L.; Fiorin, B. C. *Orbital: Electronic J. Chem.* **2025**, *17*, 234. DOI: **http://dx.doi.org/10.17807/orbital.v17i2.21049**